

# Supplementary Materials

## A novel nucleolin-binding peptide for cancer theranostics

Jae-Hyun Kim<sup>1</sup>, Chanhyung Bae<sup>2</sup>, Min-Jung Kim<sup>1</sup>, In-Hye Song<sup>1</sup>, Jae-Ha Ryu<sup>3</sup>, Jang-Hyun Choi<sup>1</sup>, Choong-Jae Lee<sup>1</sup>, Jeong-Seok Nam<sup>1,\*</sup> and Jae Il Kim<sup>1,3,\*</sup>

<sup>1</sup>School of Life Sciences, Gwangju Institute of Science and Technology, Gwangju 61005, Republic of Korea

<sup>2</sup>Molecular Physiology and Biophysics Section, Porter Neuroscience Research Center, National Institute of Neurological Disorders and Stroke, National Institutes of Health, Bethesda, United States

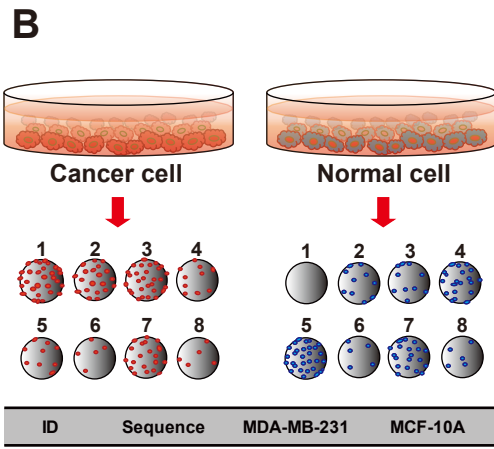
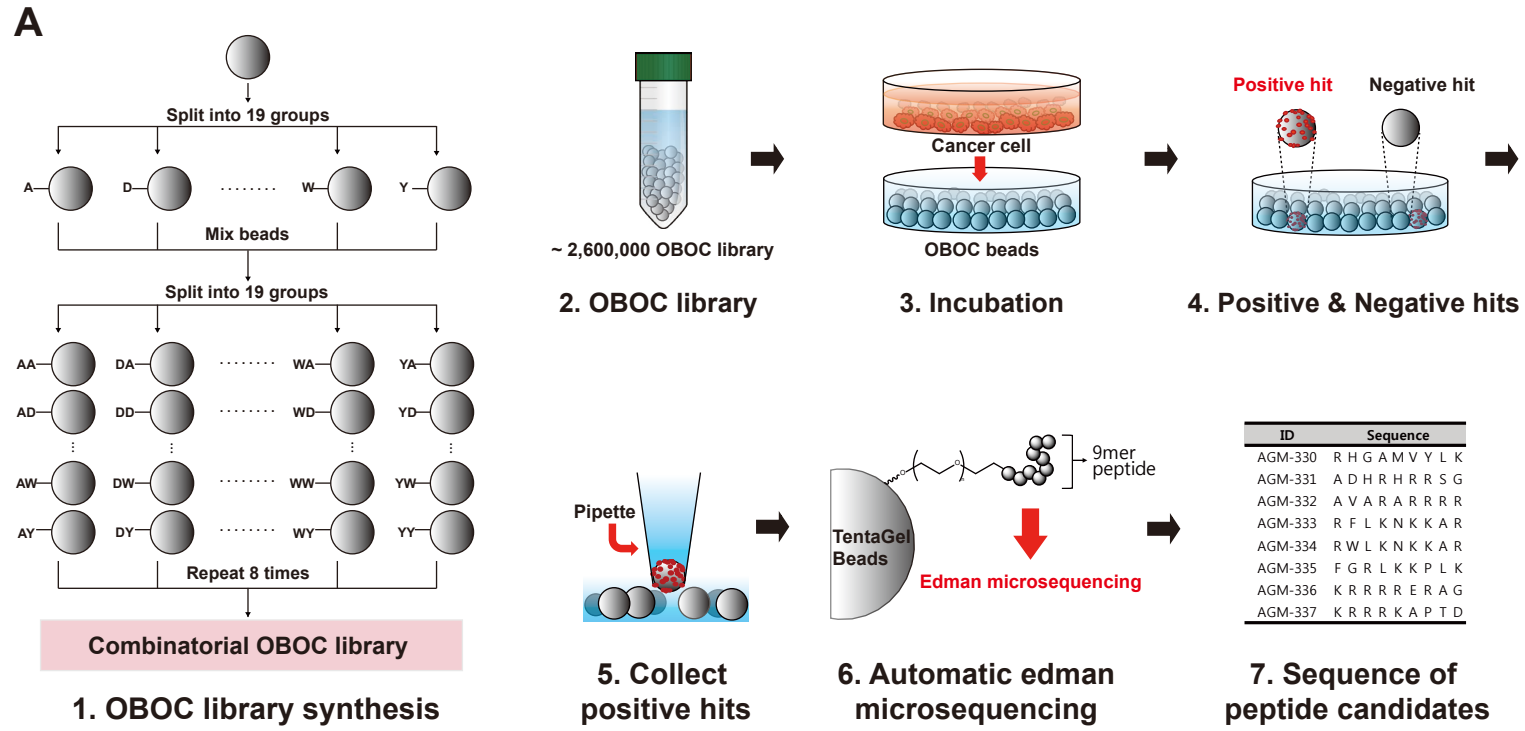
<sup>3</sup>Pilot Plant, Anygen, Gwangju, Technopark, 333 Cheomdankwagi-ro, Buk-gu, Gwangju, 61008, Republic of Korea

\*Corresponding authors

jikim@gist.ac.kr (e-mail), +82-62-715-2494 (phone), +82-62-715-2484 (fax)

namje@gist.ac.kr (e-mail), +82-62-715-2893 (phone), +82-62-715-2484 (fax)

**Figure S1**



**Note** : Semiquantitative relative binding activity: "++++" very strong binding (>40 cells per bead), "+++ " strong binding (30 -20 cells per bead), "++" moderate binding (20 - 10 cells per bead), "+" weak binding (5-10 cells per bead), "-" no binding.

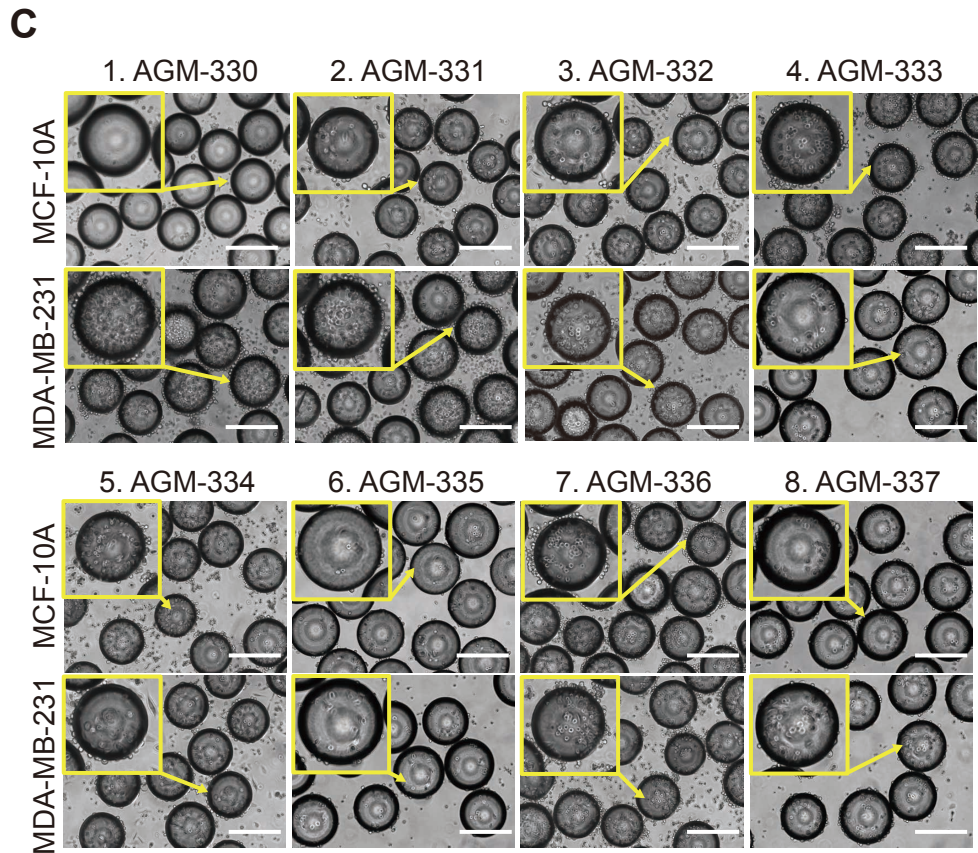
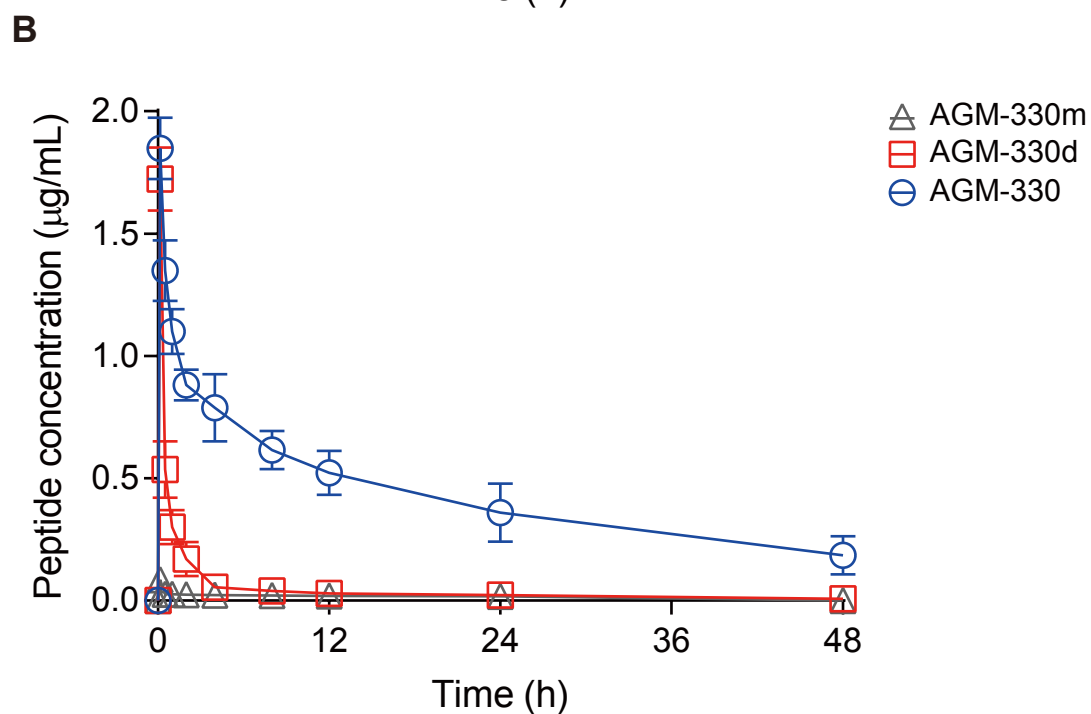
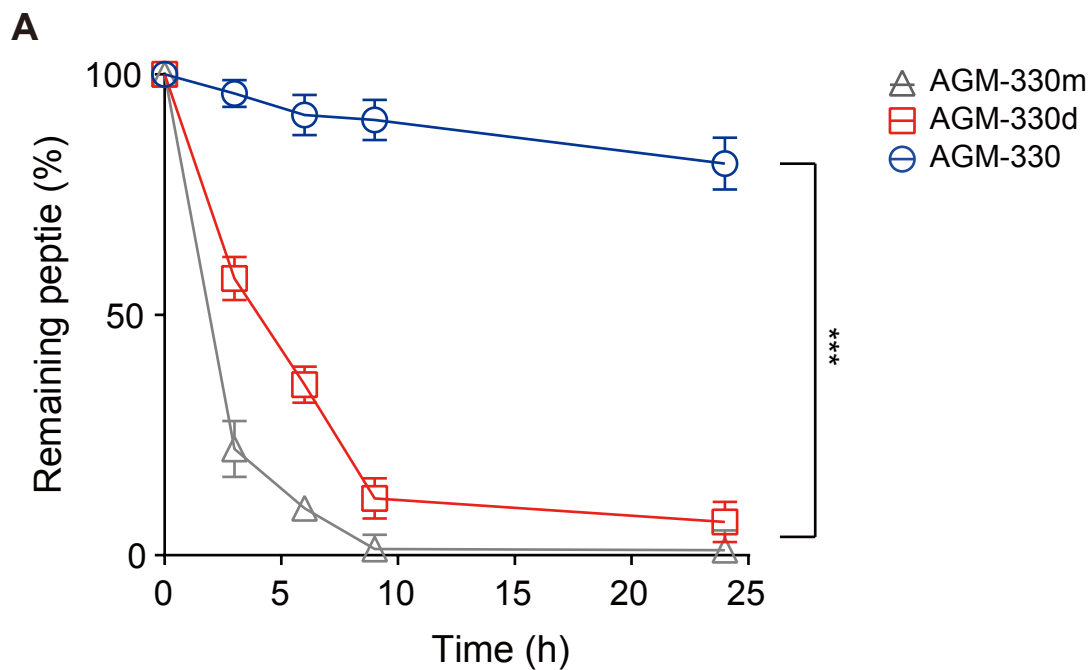


**Figure S1. A**, Steps performed in peptide library synthesis and screening. **1**, The split-mix synthesis method was performed to construct the combinatorial OBOC libraries. **2**, Approximately ~2,600,000 libraries were synthesized. **3**, OBOC libraries were incubated with cancer cells in a CO<sub>2</sub> incubator. **4**, Beads carrying ligands with an affinity for cell surface molecules became covered with cells. **5**, The positive beads were picked with a pipette under an inverted microscope. **6**, The peptide sequences for positive beads were determined by Edman microsequencing. **7**, Cancer-specific peptide ligand candidates were identified from screening OBOC combinatorial peptide libraries. **B**, The binding specificities of the peptides against cancer cell and normal cells were determined. **C**, Whole-cell binding assay results showing the cell binding specificity of 8 selected beads. Multiple breast and colorectal cancer cells and normal breast and colorectal cells were re-suspended at 10<sup>6</sup> cells/ml and incubated with beads. All experiments were repeated 3 times. Scale bar, 200 μm.

**Figure S2**



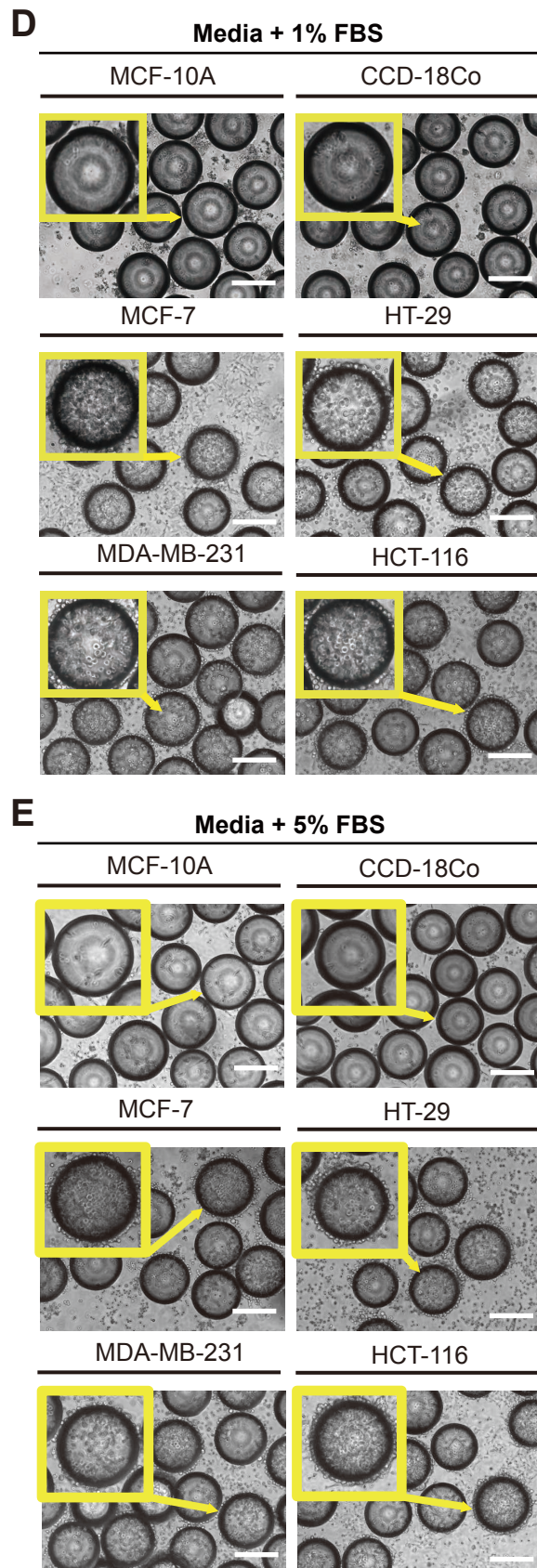
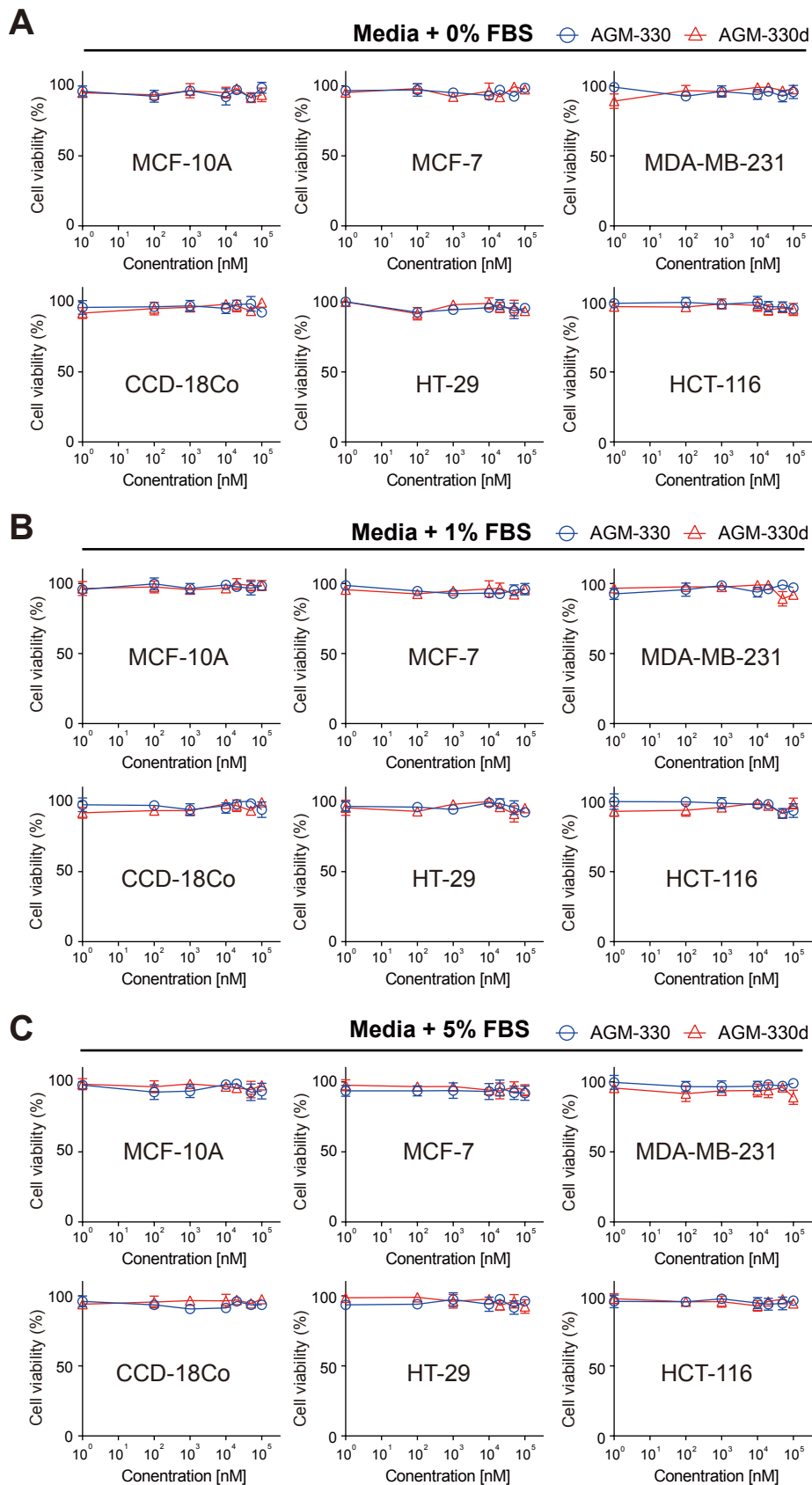
**C**

Parameters	AGM-330m	AGM-330d	AGM-330
$T_{1/2}$ (h)	$0.42 \pm 0.33$	$1.82 \pm 0.36$	$9.43 \pm 1.21$
$T_{\text{max}}$ (h)	0.167	0.167	0.167
$C_{\text{max}}$ ( $\mu\text{g/ml}$ )	$1.27 \pm 0.12$	$1.71 \pm 0.11$	$1.875 \pm 0.67$
AUC ( $\mu\text{g/h/ml}$ )	$0.64 \pm 0.09$	$1.77 \pm 0.12$	$21.42 \pm 0.81$

$T_{1/2}$ : The distribution half-time;  $T_{\text{max}}$ : Time to reach maximum plasma concentration;  $C_{\text{max}}$ : Maximum plasma concentration; AUC: Area under the plasma concentration-time curve

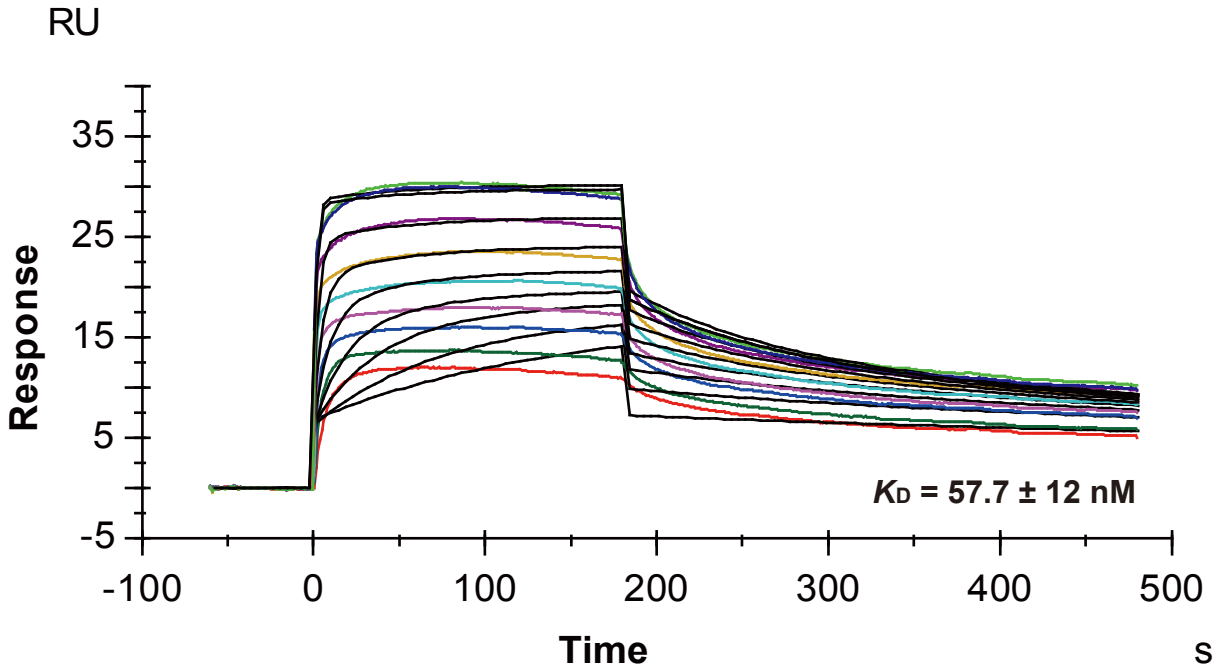
**Figure S2. A**, AGM-330m, AGM-330d and AGM-330 was incubated with pre-warmed human serum and incubated at 37 °C for 0, 3, 6, 9, and 24 h. The portion of serum-treated peptide remaining was determined by calculating the height of the respective elution peak in analytical-HPLC and comparing it with control without incubation. **B, C**, Mean plasma concentration-time profile (**B**) and pharmacokinetic parameters (**C**) of AGM-330m, AGM-330d and AGM-330 in mice ( $n = 6$ ) after single intravenous injection. Plasma peptide concentrations were quantified by ELISA, and pharmacokinetic profiles were analyzed using Phoenix WinNonlin 8.1 (*Pharsight* Corporation, Mountain View, CA, USA). The data are presented as the means  $\pm$  standard deviation. AGM-330m: Monomeric AGM-330, AGM-330d: Dimeric AGM-330, AGM-330: Tetrameric AGM-330.

**Figure S3**



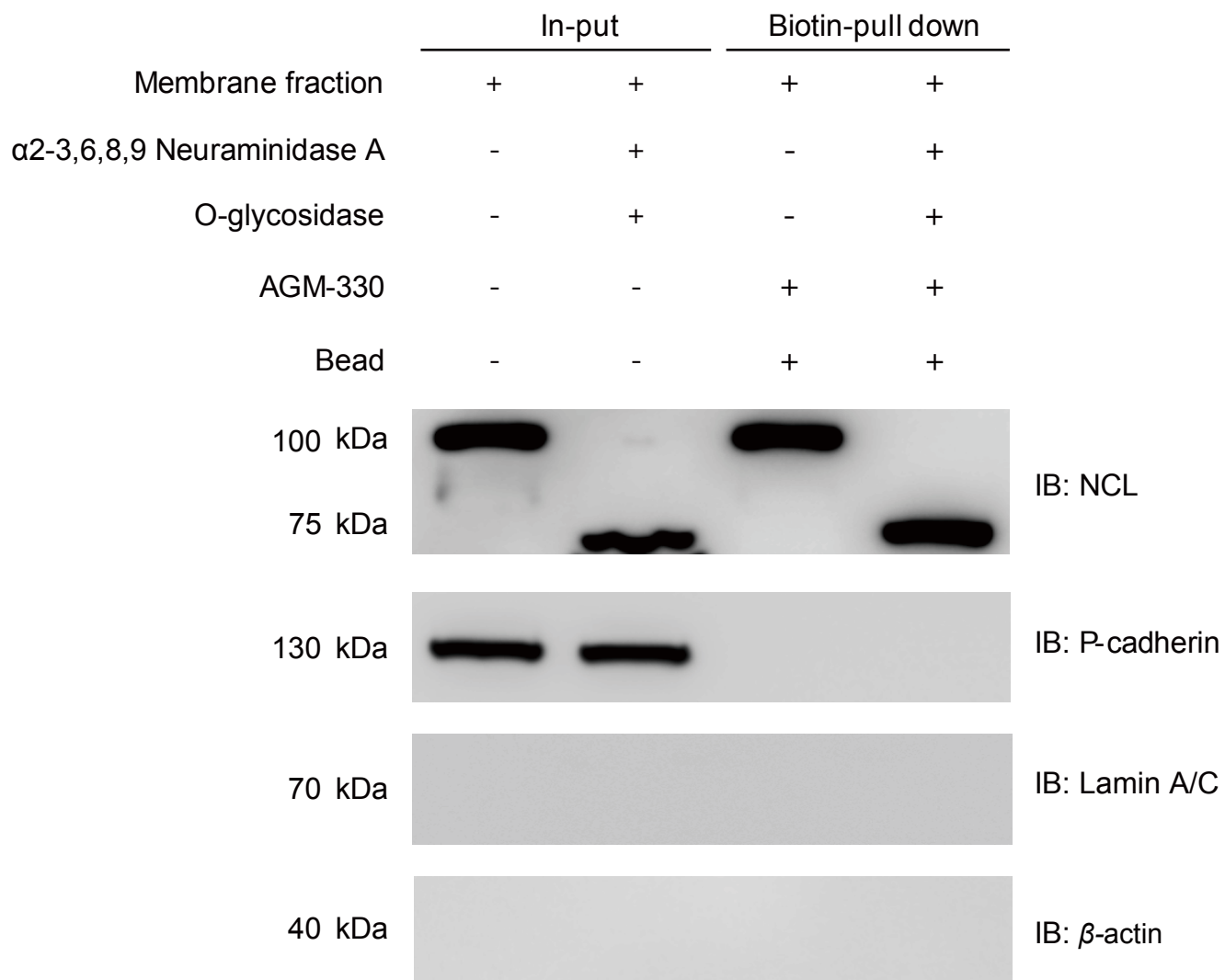
**Figure S3.** **A-C**, Cancer and normal cells ( $1 \times 10^4$  cells/well) were seeded in 96-well plates. After 24 h of incubation, the cells were treated with an increasing concentration of dimeric or tetrameric AGM-330 for 48 h. The viability of cells grown in 0 % FBS (**A**), 5 % FBS (**B**) or 10 % FBS (**C**) was assessed by a CellVia WST-1 assay (Young In Frontier, Seoul, Korea) according to the manufacturer's instruction. The numbers of viable cells were measured at a wavelength of 450 nm using an VersaMax ELISA plate reader (Molecular Devices). **D, E**, Binding specificity of AGM-330. A whole-cell binding assay was performed to determine the cell binding of AGM-330 in 1 % FBS (**D**) or 5 % FBS (**E**). Scale bar, 200  $\mu\text{m}$ .

Figure S4



**Figure S4.** AGM-330 affinity for recombinant NCL was assessed by SPR using an increasing concentration (20 nM - 2.5  $\mu$ M) of AGM-330. The SPR sensorgrams shown are from an experiment that is representative of a set of three separate experiments using different sensor chips with similar results. Recombinant NCL was immobilized onto a CM5 sensorchip. Different concentrations of AGM-330 were incubated with immobilized NCL and analyzed on a Biacore T-200 apparatus. The resulting  $K_D$  values are also indicated.

**Figure S5**



**Figure S5.** Analysis of the interaction between AGM-330 and *O*-glycan-cleaved membrane NCL by a biotin pull-down assay. Immunoblotting analysis of the eluted proteins from the biotin pull-down using an anti-NCL antibody. Lane 1: Input of membrane NCL; Lane 2: Input of *O*-glycan-cleaved membrane NCL; Lane 3: Elution after incubation with membrane NCL; Lane 4: Elution after incubation with *O*-glycan-cleaved membrane NCL.

Figure S6

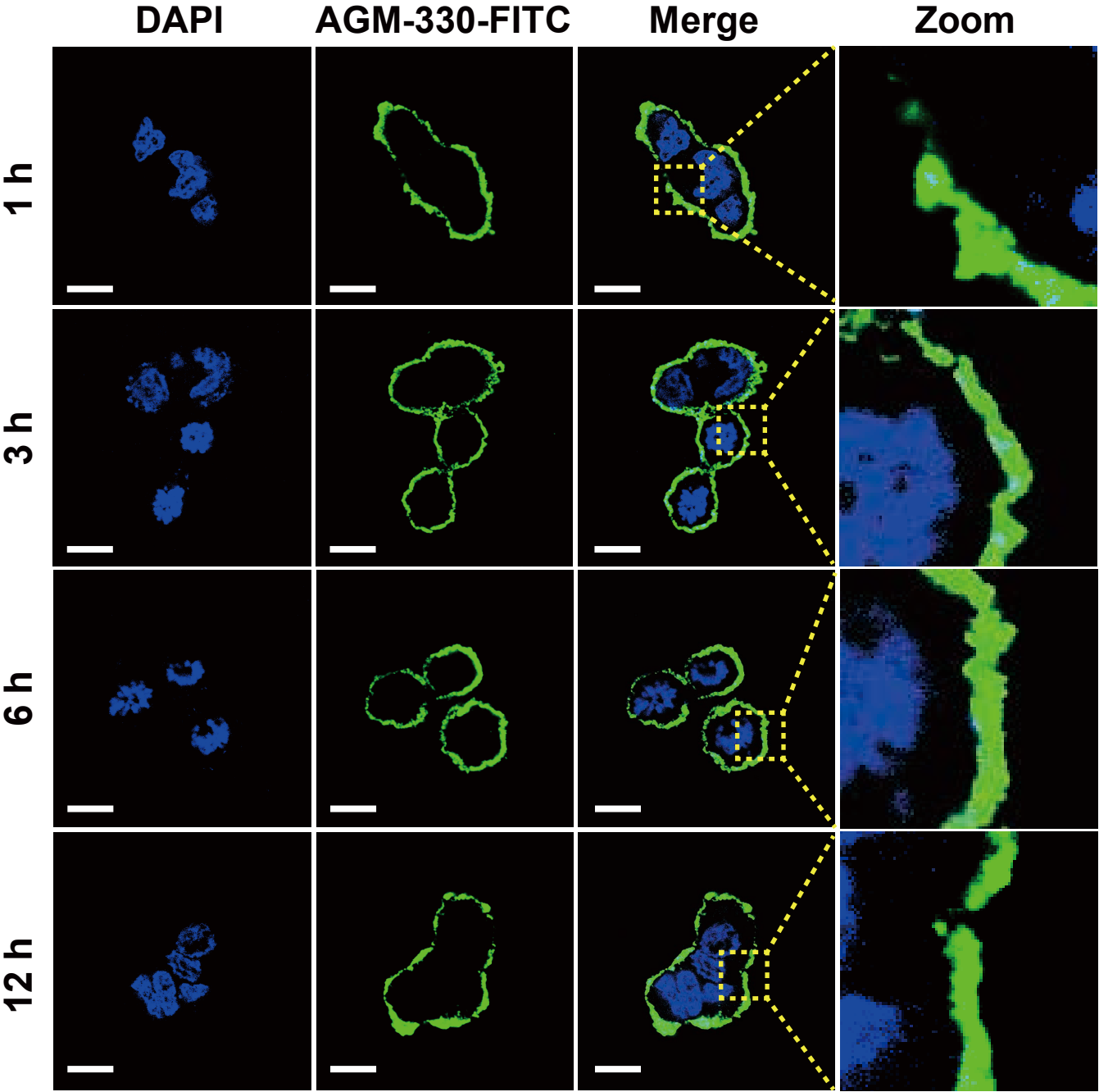
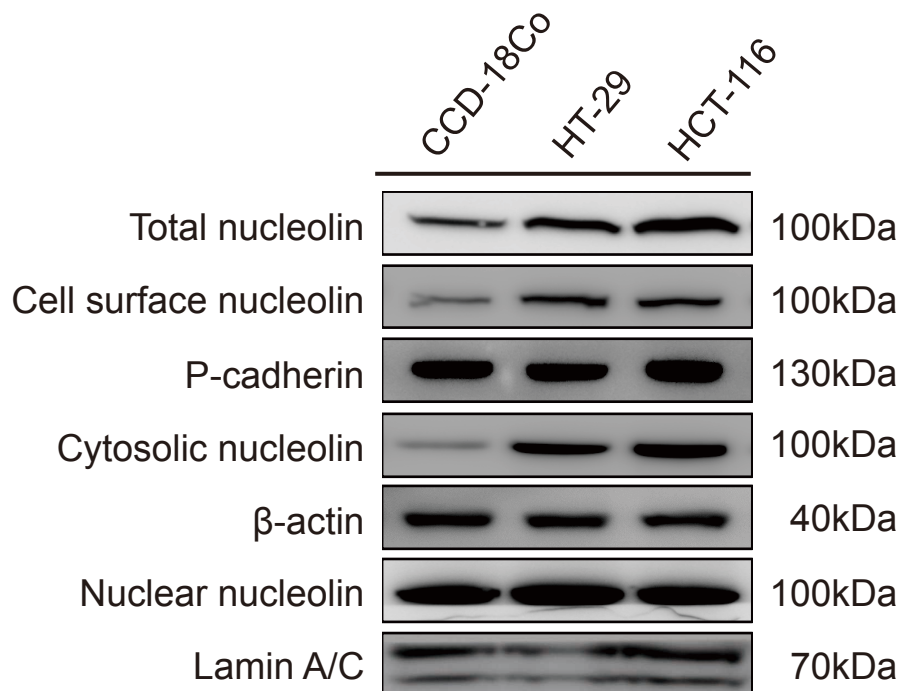


**Figure S6.** Time-dependent *in vitro* binding assay of AGM-330-FITC toward cancer cells. MDA-MB-231 cells were incubated with 5  $\mu\text{mol/l}$  AGM-330-FITC for 1, 3, 6 and 12 h at 37 °C. The cells were then fixed with 4 % paraformaldehyde, and the nuclei were stained with DAPI. MERGE represents a merged image of AGM-330-FITC and nuclear staining by DAPI. AGM-330-FITC: FITC-conjugated AGM-330. Scale bar, 20  $\mu\text{m}$ .

Figure S7

A



B

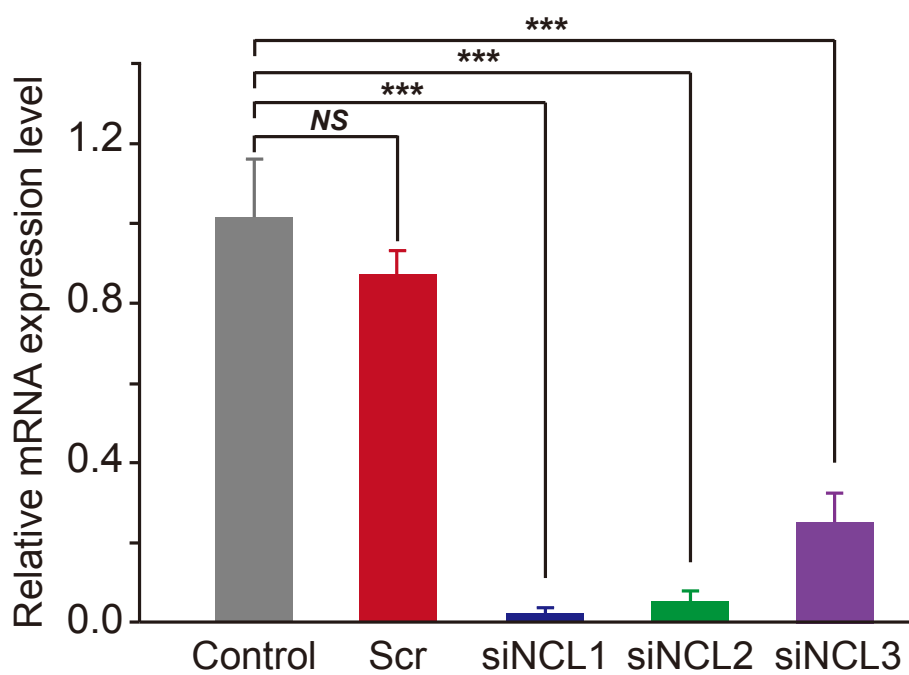
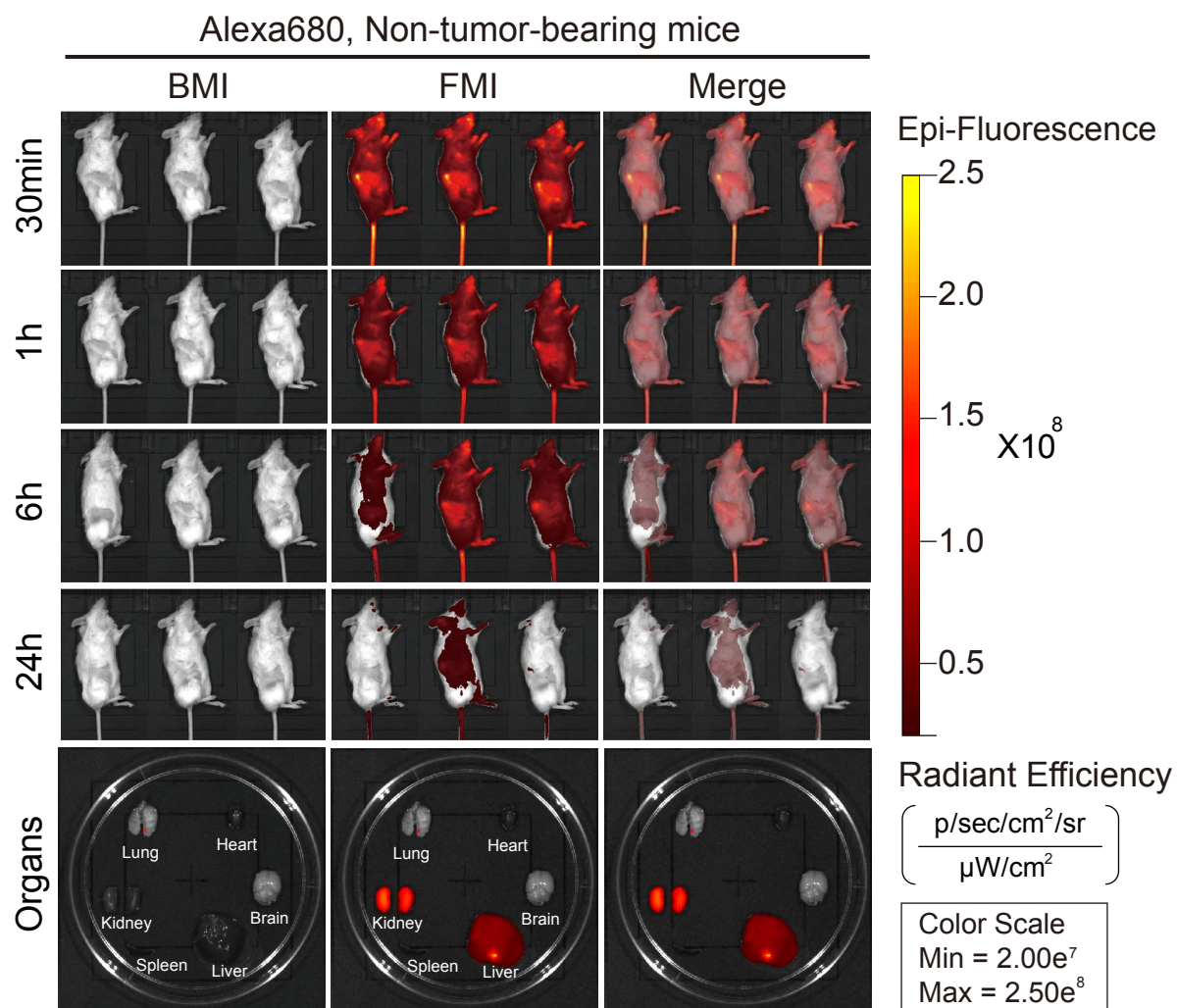


Figure S7

C



**Figure S7. A**, The NCL distribution in various subcellular fractions was analyzed in CCD-18Co, HT-29, and HCT-116 cells. Plasma membrane, cytosol and nuclear NCL were immunoblotted using an anti-NCL antibody. **B**, MDA-MB-231 cells were transfected with non-targeting scrambled siRNA (Scr) or NCL-targeting siNCL1, siNCL2, or siNCL3. After 24 h, the efficiencies of gene silencing were determined by real-time PCR. Based on the observed mRNA levels, one set of siRNAs (siNCL1) showed significant target gene knockdown efficiency and was used in further experiments. **C**, *In vivo* fluorescence images of mice 30 min, 1 h, 6 h, and 24 h after intravenous injections of 10 nmol free Alexa680 in non-tumor-bearing mice. Fluorescence images of the major organs, including the heart, spleen, lung, brain, liver, kidney, and tumors removed from mice with different treatments. The bar graphs show the means  $\pm$  SD, and statistical analyses were performed using one-way ANOVA with Dunnett's multiple comparison. \*, \*\*, and \*\*\* indicate  $P < 0.05$ ,  $P < 0.01$ , and  $P < 0.001$ , respectively.

**Figure S8**

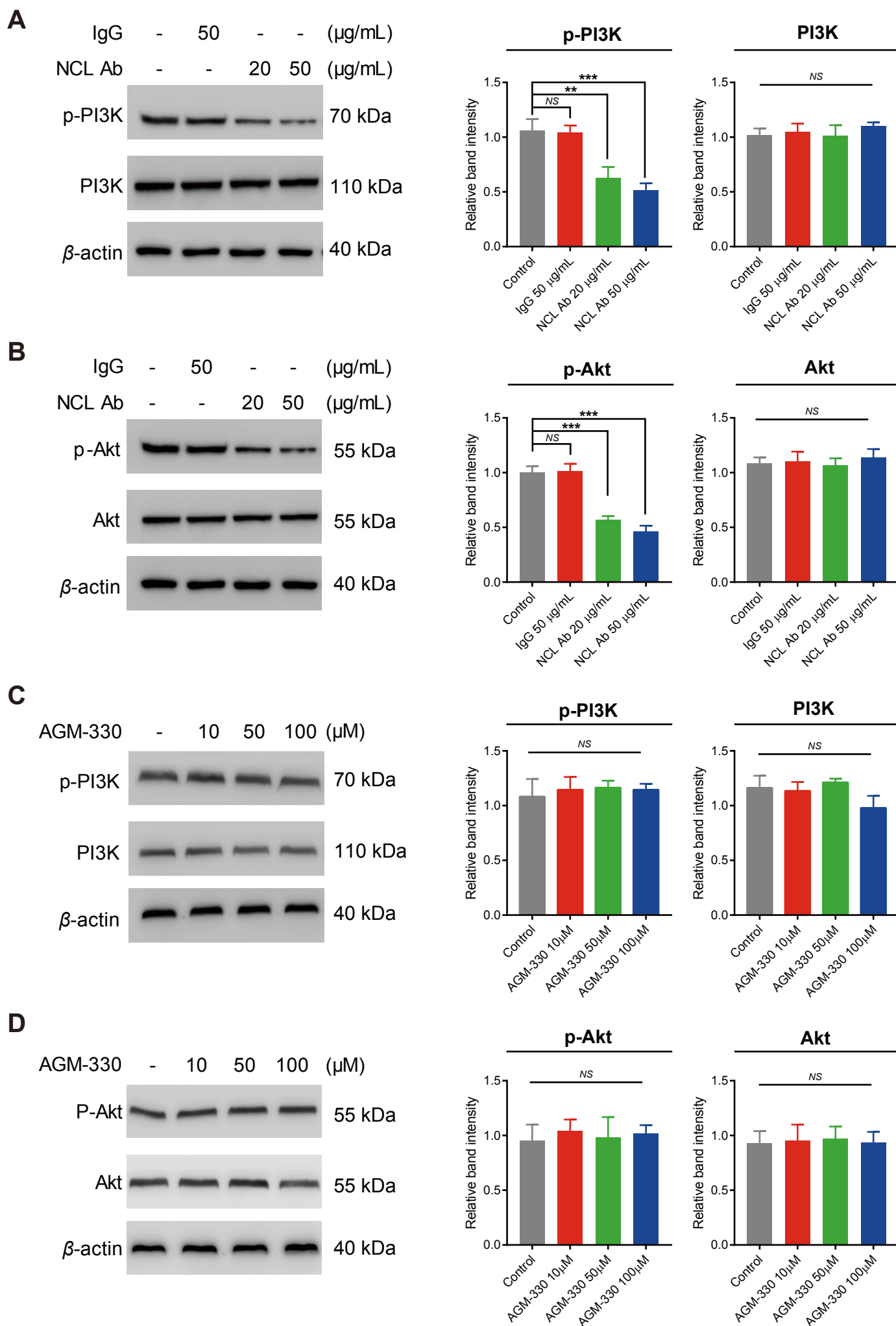
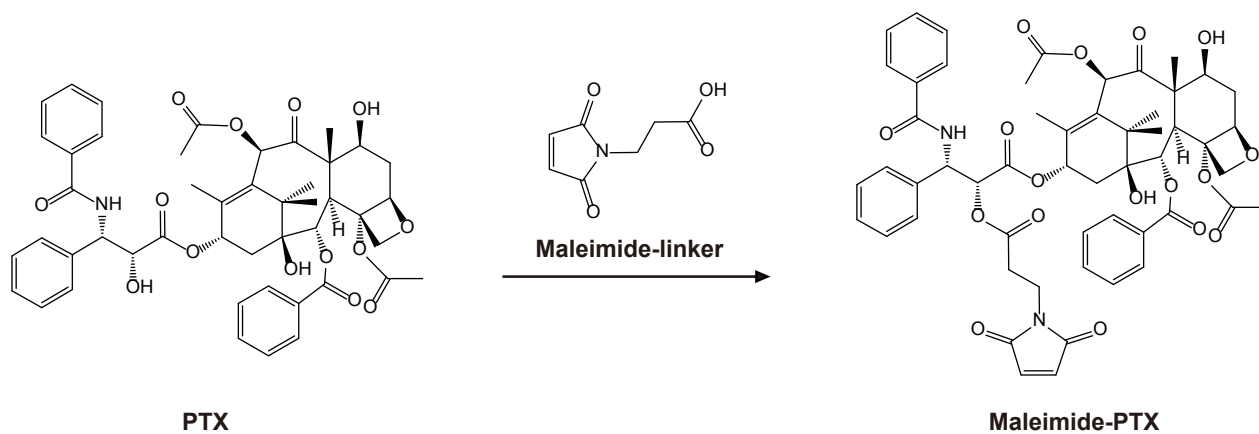


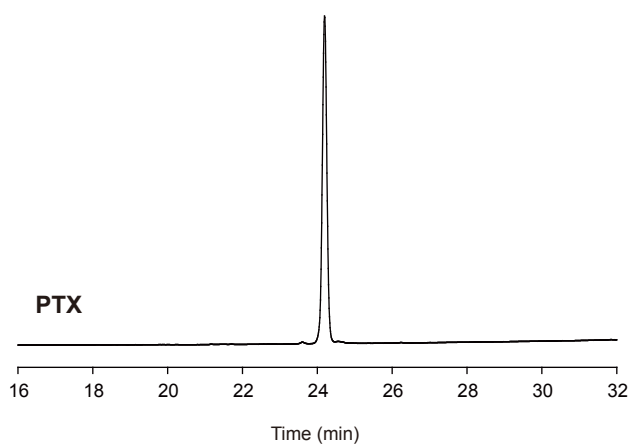
**Figure S8. A-D**, Western blot analysis of PI3K/Akt signaling in MDA-MB-231 cells stimulated by increasing concentrations of an anti-NCL antibody and AGM-330. After treatment with the anti-NCL antibody (**A,B**) or AGM-330 (**C,D**), the protein levels of p-PI3K, PI3K, p-Akt and Akt were assessed by immunoblot analysis. The bar graphs show the means  $\pm$  SD, and statistical analyses were performed using one-way ANOVA with Dunnett's multiple comparison. \*, \*\*, and \*\*\* indicate  $P < 0.05$ ,  $P < 0.01$ , and  $P < 0.001$ , respectively.

**Figure S9**

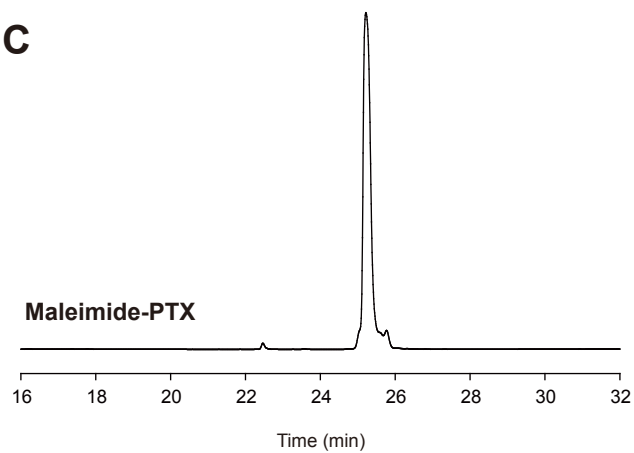
**A**



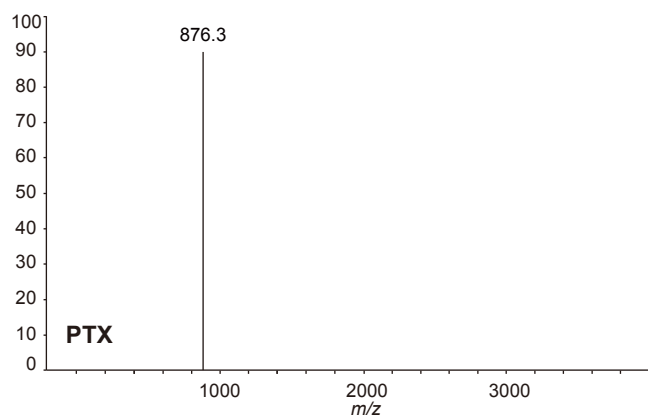
**B**



**C**



**D**



**E**

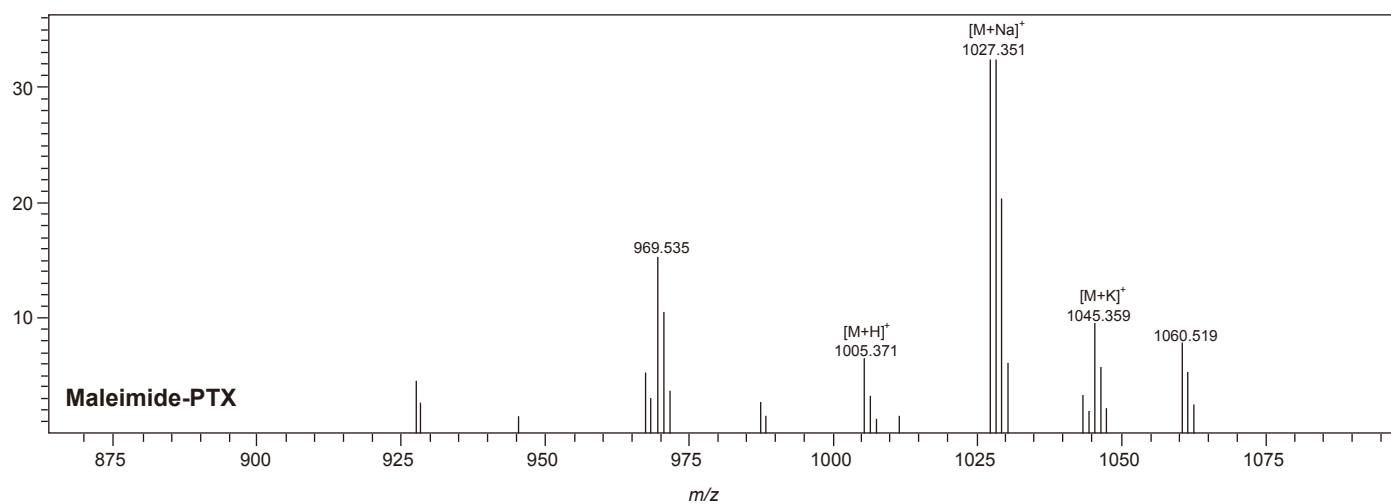
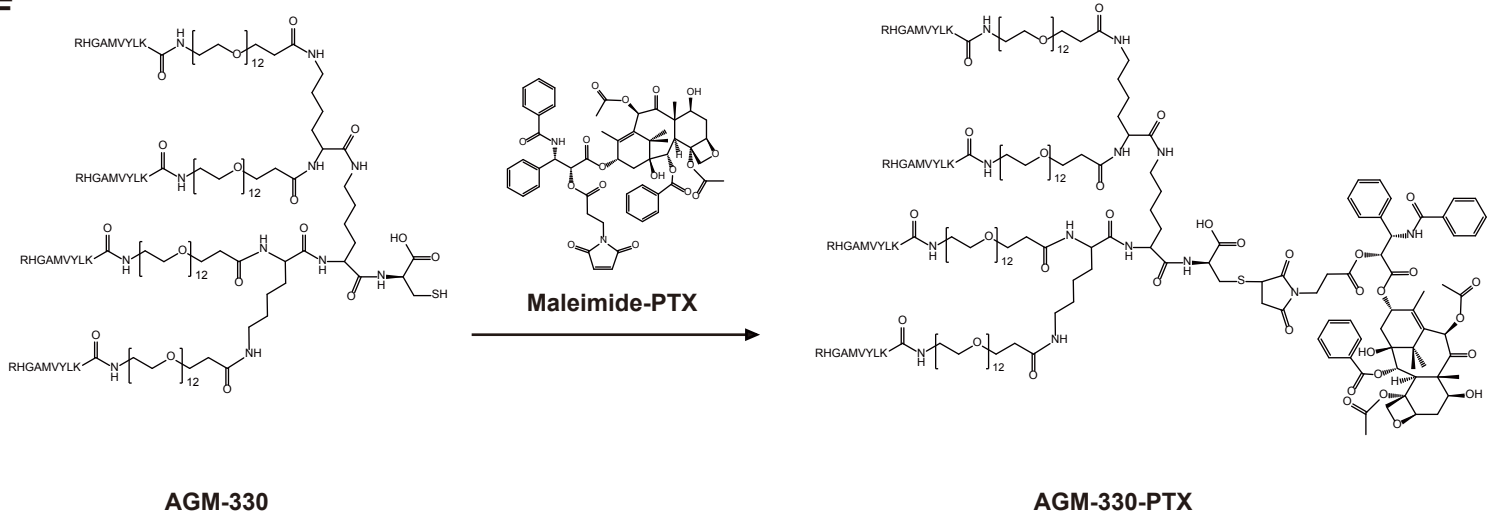
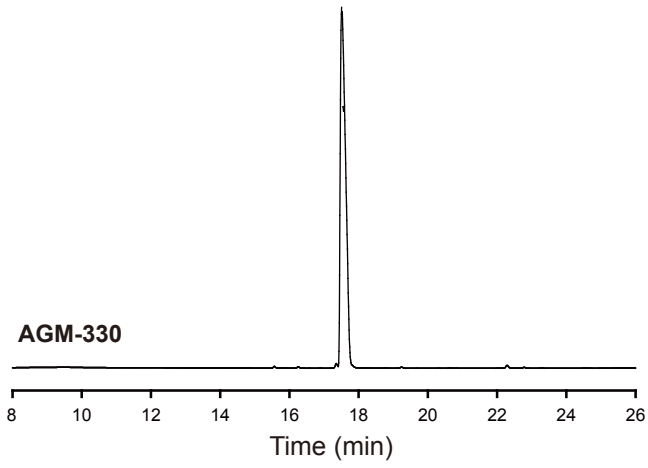


**Figure S9**

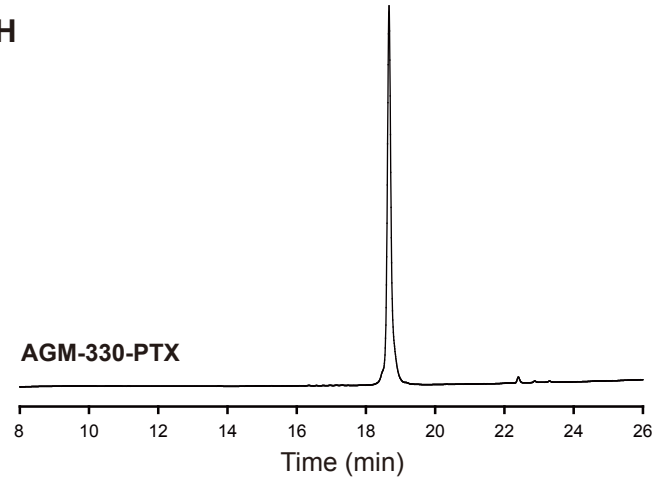
**F**



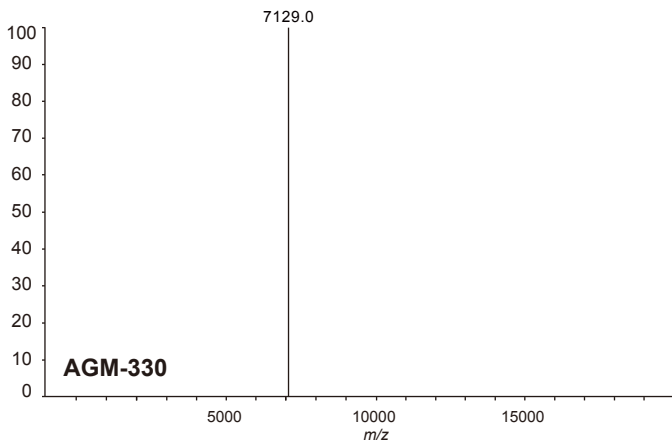
**G**



**H**



**I**



**J**

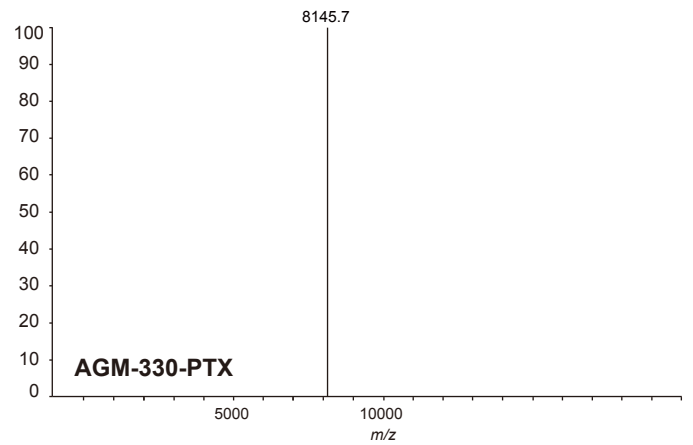
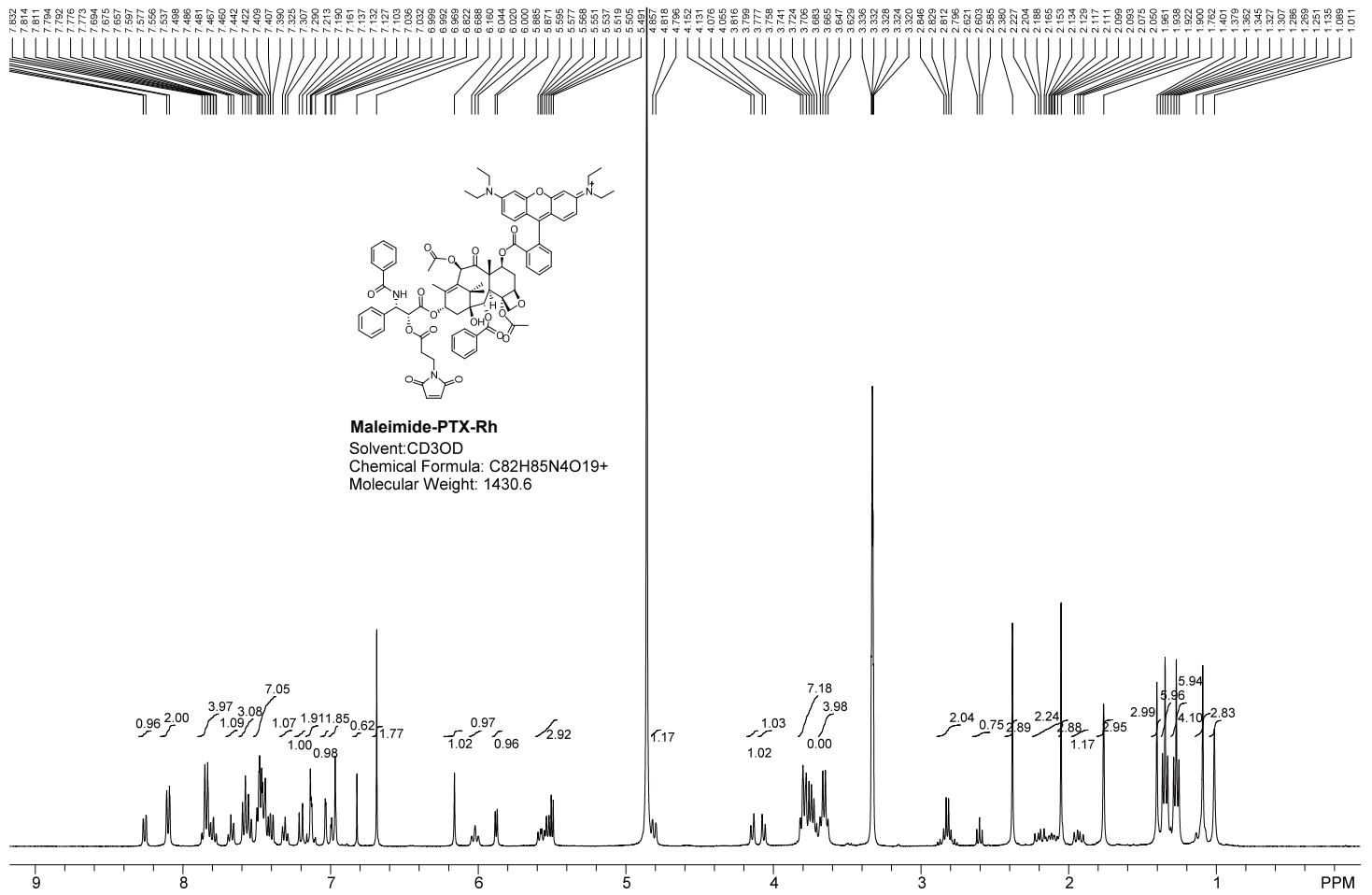
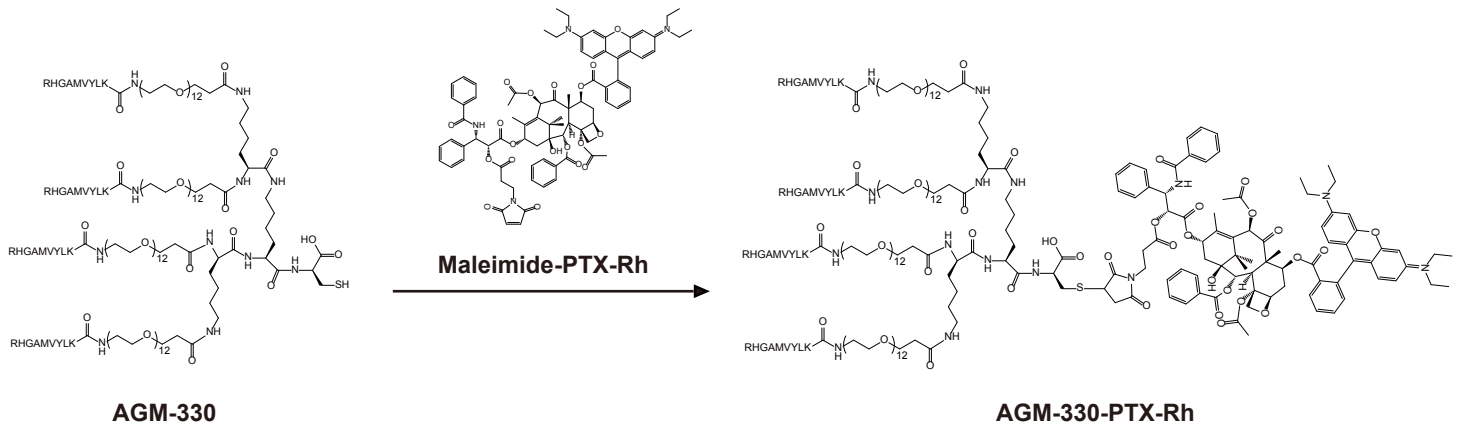


Figure S9

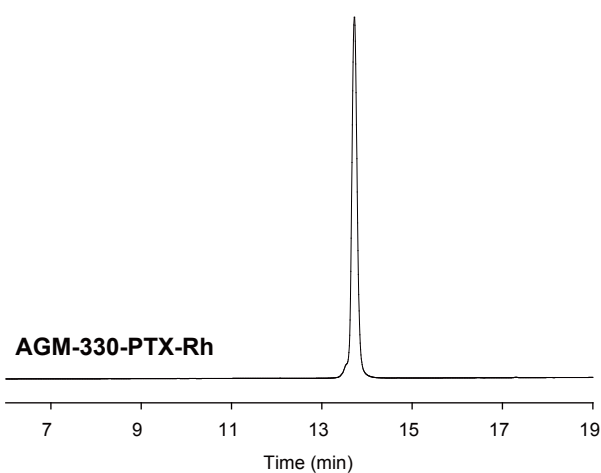
K



L



M



N

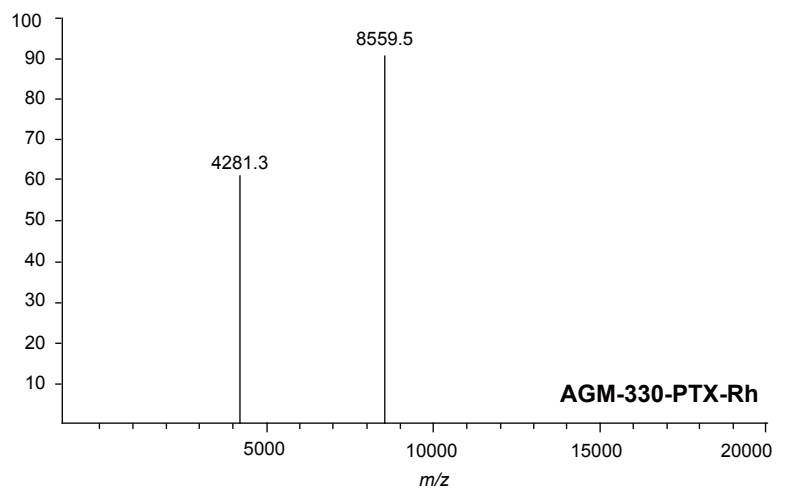


**Figure S9.** **A**, Conjugation of paclitaxel (PTX) with a maleimide linker. **B-E**, HPLC chromatograms and MS spectra of PTX and maleimide-PTX. The HPLC chromatograms of PTX (**B**) and maleimide-PTX (**C**). MS spectra of PTX (**D**) by MALDI-TOF and maleimide-PTX (**E**) by ESI-MS. **F**, Conjugation of AGM-330 with maleimide-PTX. **G-J**, HPLC chromatograms and MS spectra of AGM-330 and AGM-330-PTX. The HPLC chromatograms of AGM-330 (**G**) and AGM-330-PTX (**H**). MS spectra of AGM-330 (**I**) and AGM-330-PTX (**J**) by MALDI-TOF. **K**, <sup>1</sup>H-NMR spectra of maleimide-PTX-Rh. <sup>1</sup>H-NMR: (400 MHz, CD<sub>3</sub>OD): δ 8.27 (d, *J* = 0.8Hz, 1H), 8.25-8.11 (m, 2H), 8.09-7.77 (m, 4H), 7.69-7.65 (m, 1H), 7.59-7.53 (m, 3H), 7.49-7.39 (m, 7H), 7.31 (t, *J* = 7.2Hz, 1H), 7.20 (d, *J* = 9.2Hz, 1H), 7.13-7.10 (m, 2H), 7.03 (d, *J* = 0.8Hz, 1H), 6.99-6.95 (m, 2H), 6.82-6.68 (m, 2H), 6.16 (s, 1H), 6.02 (t, *J* = 8Hz, 1H), 5.87 (d, *J* = 6Hz, 1H), 5.59-5.49 (m, 3H), 4.80 (d, *J* = 8.8Hz, 1H), 4.14 (d, *J* = 8.4Hz, 1H), 4.06 (d, *J* = 8.4Hz, 1H), 3.82-3.70 (m, 7H), 3.68-3.63 (m, 4H), 2.84-2.79 (m, 2H), 2.60 (t, *J* = 7.2Hz, 1H), 2.38 (s, 3H), 2.22-2.07 (m, 2H), 2.05 (s, 3H), 1.96-1.90 (m, 1H), 1.76 (s, 3H), 1.40 (s, 3H), 1.37-1.25 (m, 12H), 1.13-1.08 (m, 4H), 1.01 (s, 3H). **L**, Conjugation of AGM-330 with maleimide-PTX-Rh. **M**, **N**, HPLC chromatogram (**M**) and MS spectrum (**N**) of AGM-330-PTX-Rh. Maleimide-PTX: maleimide-linker conjugated PTX; AGM-330-PTX: maleimide-PTX conjugated AGM-330; maleimide-PTX-Rh: rhodamine B conjugated maleimide-PTX; AGM-330-PTX-Rh: maleimide-PTX-Rh conjugated AGM-330.

**Figure S10**

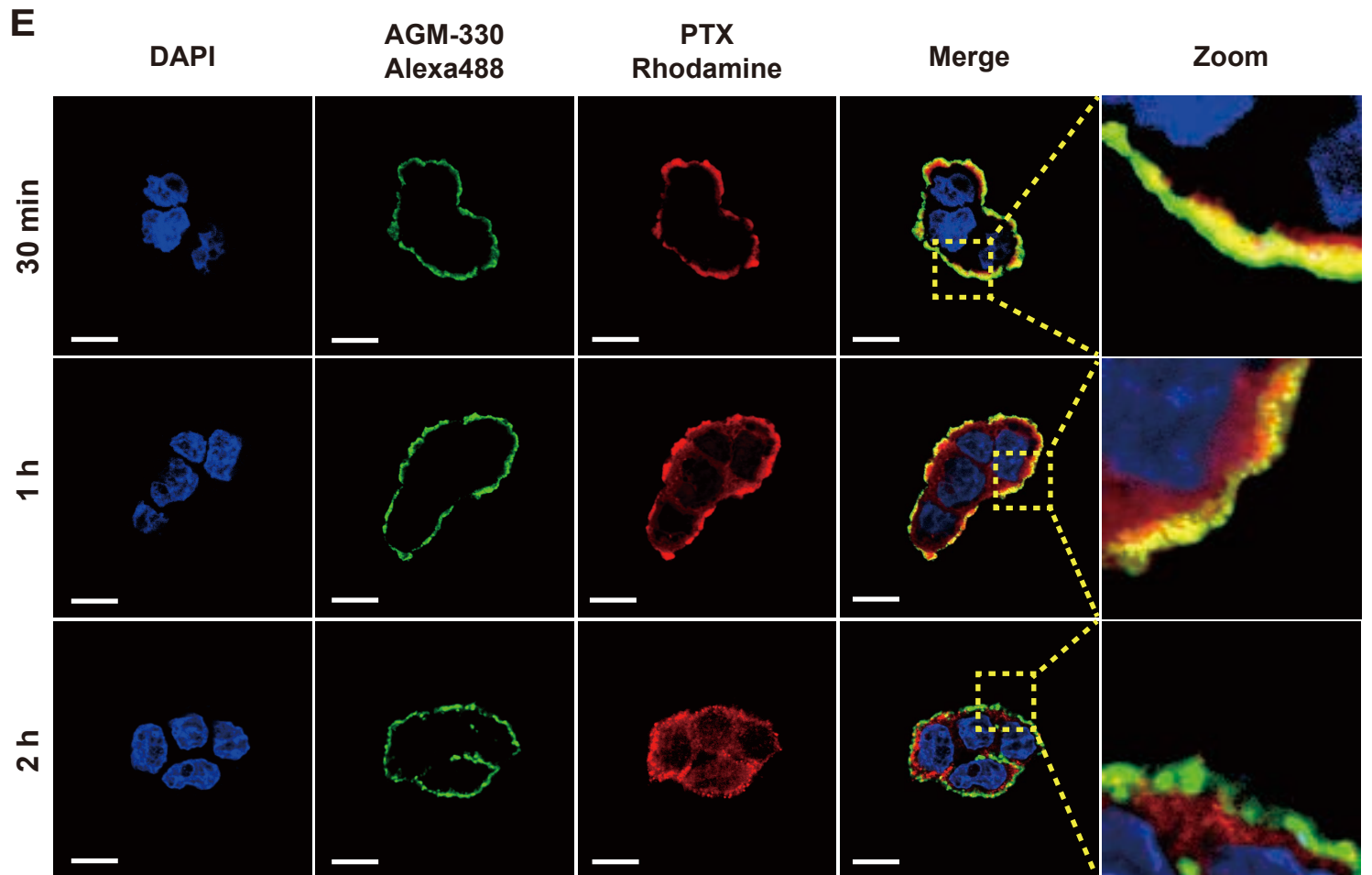
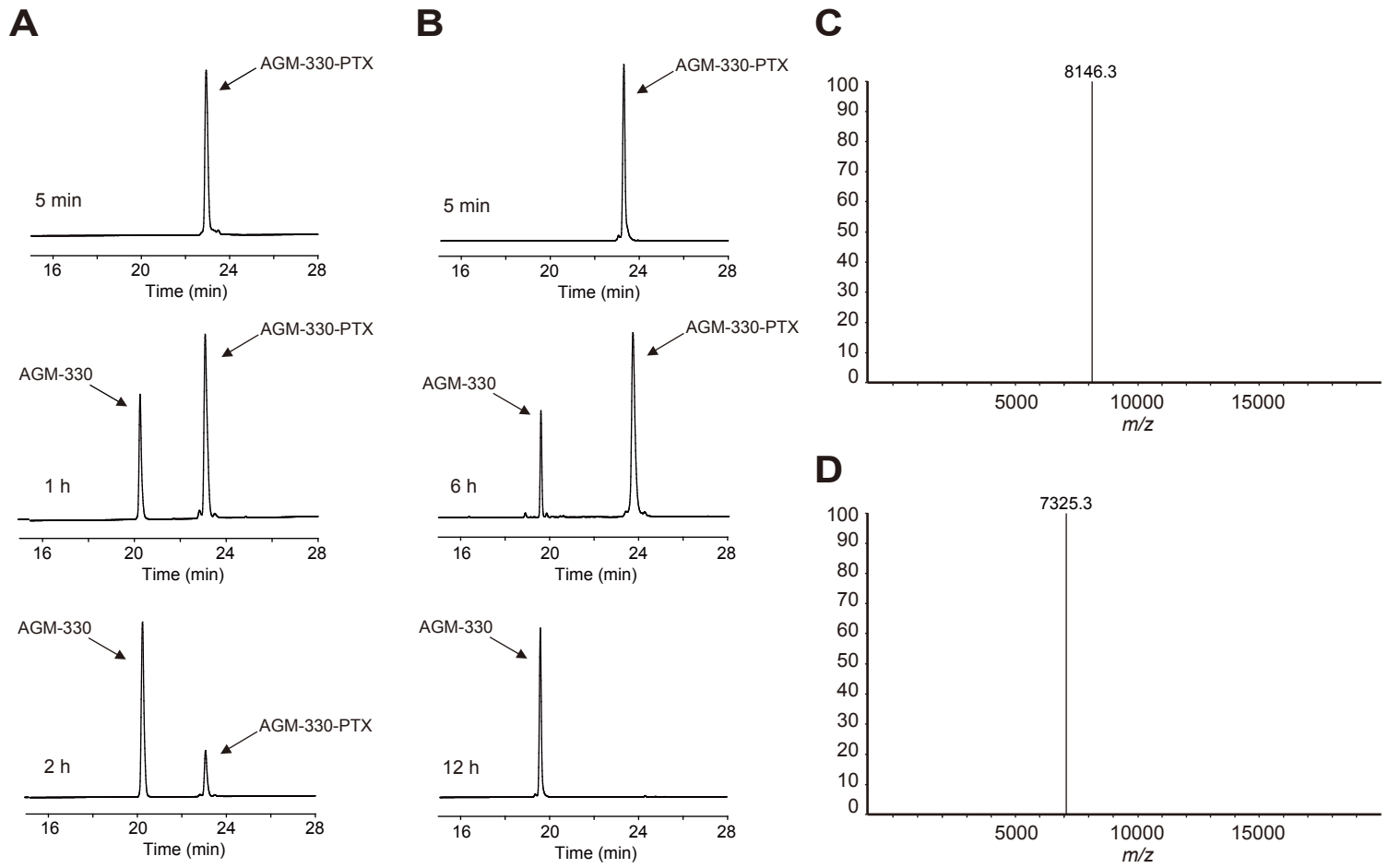


**Figure S10.** **A, B**, Changes in the HPLC chromatogram of AGM-330-PTX after incubation with human serum (**A**) or PBS (**B**). **C, D**, MS spectra of AGM-330-PTX (**C**) and AGM-330 (**D**). **E**, Time-dependent fluorescence imaging of AGM-330-PTX-Rh in MDA-MB-231 cells. Cells were incubated with 5  $\mu\text{mol/l}$  AGM-330-PTX-Rh. AGM-330 was stained with a primary anti-AGM-330 antibody, and the complex was revealed using an anti-rabbit secondary antibody coupled to Alexa Fluor 488. Cells were then fixed with 4 % paraformaldehyde, and the nuclei were stained with DAPI. MERGE represents a merged image of AGM-330, PTX, and nuclear staining by DAPI. Scale bar, 20  $\mu\text{m}$ .

Figure S11

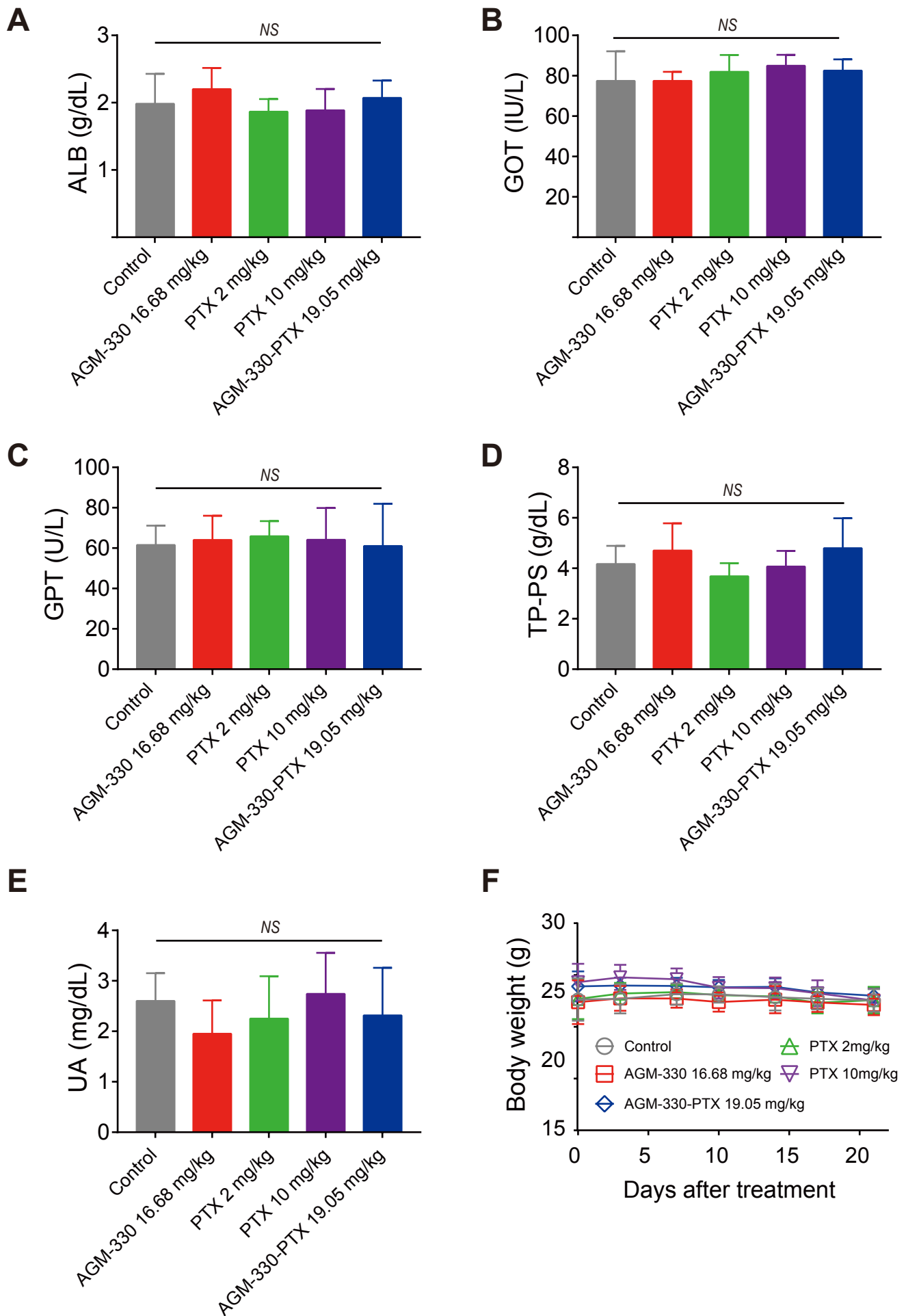


**Figure S11. A-E**, NPG<sup>TM</sup> mice bearing MDA-MB-231-luc tumors were treated twice a week for 21 days with intravenous doses of vehicle (PBS), PTX (2 or 10 mg/kg), AGM-330 (16.68 mg/kg, molar equivalent to 2 mg/kg PTX) and AGM-330-PTX (19.05 mg/kg, molar equivalent to 2 mg/kg PTX) ( $n = 5$ ). Blood was collected from xenografted mice under isoflurane-induced deep anesthesia by cardiac puncture. After allowing for blood coagulation at 4 °C, serum was collected by centrifugation at 3000 rpm for 10 min at 4 °C. Analysis of the levels of (A), ALB, (B), GOT, (C), GPT, (D), TP-PS, and (E), UA in the serum was performed using a veterinary hematology analyzer (Fuji DRI-Chem 3500 s, Fujifilm, Tokyo, Japan) according to the manufacturer's provided protocols. ALB, albumin; GOT, glutamic oxaloacetic transaminase; GTP, glutamate pyruvate transaminase; TP-PS, total protein/protein scan; UA, uric acid. **F**, Body weight changes after 3 weeks of different treatments indicated in xenograft mice. AGM-330d-PTX: PTX-conjugated dimeric AGM-330. The bar graphs show the means  $\pm$  SD, and statistical analyses were performed using one-way ANOVA with Dunnett's multiple comparison. \*, \*\*, and \*\*\* indicate  $P < 0.05$ ,  $P < 0.01$ , and  $P < 0.001$ , respectively.A



**Figure S12.** **A**, Structure of AGM-330d-PTX. **B**, Schematic representation of the experimental protocol as described in the Materials and Methods section. Anesthetized 6 week-old male NPG mice were inoculated with a 1:1 mix of Matrigel and  $1 \times 10^6$  MDA-MB-231-luc cells into the mammary fat pad. When the volume of the primary tumors reached approximately  $100 \text{ mm}^3$ , tumor-bearing mice were treated with vehicle (PBS), PTX (2 or 10 mg/kg), AGM-330d (8.34 mg/kg, molar equivalent to 2 mg/kg PTX), or AGM-330d-PTX (10.71 mg/kg, molar equivalent to 2 mg/kg PTX) ( $n = 5/\text{group}$ ). **C**, Monitoring of tumor growth through whole-body bioluminescence imaging. The mice were subjected to bioluminescence imaging every 5 days. **D**, Bioluminescence was quantified for each time point using the region of interest tool in the Living Image software program. **E-G**, The therapeutic effect of AGM-330d-PTX was evaluated in breast cancer xenograft models. MDA-MB-231-luc cells were subcutaneously inoculated into the mammary fat pads of NPG mice. **(E)**, The primary tumor volume was measured twice per week until the day of sacrifice. The primary tumor volume was calculated using the following formula:  $\text{volume (mm}^3) = [\text{length (mm)}] \times [\text{width (mm)}]^2 \times 0.5$ . **(F)**, On the day of sacrifice, all primary tumors were isolated, and **(G)** the primary tumor weights were evaluated. **H**, Body weight changes after 3 weeks of different treatments in the indicated xenograft mice. AGM-330d-PTX: PTX-conjugated dimeric AGM-330. Bar graphs represent the means  $\pm$  SD, and statistical analyses were performed using one-way ANOVA with Dunnett's multiple comparison. \*, \*\*, and \*\*\* indicate  $P < 0.05$ ,  $P < 0.01$ , and  $P < 0.001$ , respectively.